Published in final edited form as:
J Neural Transm. 2014 February ; 121(2): 171–181. doi:10.1007/s00702-013-1084-z.

A QUANTITATIVE STUDY OF α-SYNUCLEIN PATHOLOGY IN FIFTEEN CASES OF DEMENTIA ASSOCIATED WITH PARKINSON DISEASE

Richard A. Armstrong[1,*], **Paul T. Kotzbauer**[2,3,4], **Joel S. Perlmutter**[2,4,5,6,7,8], **Meghan C. Campbell**[2,5], **Kyle M. Hurth**[9], **Robert E. Schmidt**[9], and **Nigel J. Cairns**[2,4,9,10]

[1]Vision Sciences, Aston University, Birmingham, B4 7ET, UK

[2]Department of Neurology, Washington University School of Medicine, St. Louis, MO, USA

[3]Department of Developmental Biology, Washington University School of Medicine, St. Louis, MO, USA

[4]Hope Center for Neurological Disorders, Washington University School of Medicine, St. Louis, MO, USA

[5]Department of Radiology, Washington University School of Medicine, St. Louis, MO, USA

[6]Department of Anatomy & Neurobiology, Washington University School of Medicine, St. Louis, MO, USA

[7]Program in Occupational Therapy, Washington University School of Medicine, St. Louis, MO, USA

[8]Program in Physical Therapy, Washington University School of Medicine, St. Louis, MO, USA

[9]Department of Pathology & Immunology, Washington University School of Medicine, St. Louis, MO, USA

[10]Knight Alzheimer's Disease Research Center, Washington University School of Medicine, St. Louis, MO, USA

Abstract

The α-synuclein-immunoreactive pathology of dementia associated with Parkinson disease (DPD) comprises Lewy bodies (LB), Lewy neurites (LN), and Lewy grains (LG). The densities of LB, LN, LG together with vacuoles, neurons, abnormally enlarged neurons (EN), and glial cell nuclei were measured in fifteen cases of DPD. Densities of LN and LG were up to 19 and 70 times those of LB respectively, depending on region. Densities were significantly greater in amygdala, entorhinal cortex (EC), and sectors CA2/CA3 of the hippocampus, whereas middle frontal gyrus (MFG), sector CA1, and dentate gyrus were least affected. Low densities of vacuoles and EN were recorded in most regions. There were differences in the numerical density of neurons between regions but no statistical difference between patients and controls. In the cortex, the density of LB and vacuoles was similar in upper and lower laminae while the densities of LN and LG were

Corresponding Author: R.A. Armstrong, Vision Sciences, Aston University, Birmingham, B4 7ET, UK (Tel 0121-359-3611; Fax 0121-333-4220; R.A.Armstrong@aston.ac.uk).

greater in upper cortex. The densities of LB, LN, and LG were positively correlated. Principal components analysis (PCA) suggested DPD cases were heterogeneous with pathology primarily affecting either hippocampus or cortex. The data suggest in DPD: (1) ratio of LN and LG to LB varies between regions, (2) low densities of vacuoles and EN are present in most brain regions, (3) degeneration occurs across cortical laminae, upper laminae being particularly affected, (4) LB, LN and LG may represent degeneration of the same neurons, and (5) disease heterogeneity may result from variation in anatomical pathway affected by cell to cell transfer of α-synuclein.

Keywords

Parkinson disease with dementia (DPD); α-Synuclein; Lewy bodies (LB); Lewy neurites (LN); Lewy grains (LG); Principal components analysis (PCA)

Introduction

Parkinson disease (PD) (all abbreviations used in the text are listed in Table 1), a chronic neurodegenerative disorder, results in a variety of movement problems including bradykinesia, rigidity, tremor, and postural instability. Non-motor symptoms, however, also play a significant role in determining the quality of life of the patient (Antal et al 1998, Armstrong 2008). Hence, cognitive decline in PD can range from subtle mental dysfunction to overt dementia (Braak et al 2005). Dementia associated with PD (DPD) is a particularly debilitating condition substantially increasing mortality (Willis et al 2012). The risk of DPD increases with patient age, 90% of recorded cases being over 70 years of age (Rana et al 2012).

DPD patients exhibit reduced gray matter volume in several brain regions including temporal cortex, most notably the parahippocampal gyrus (PHG), parietal and frontal cortices, cingulate gyrus (CG), caudate nucleus, hippocampus, amygdala, and putamen (Melzer et al 2012). Histologically, PD is characterized by the death of pigmented neurons in the substantia nigra (SN), neurons of the SN and cerebral cortex containing α-synuclein-immunoreactive neuronal cytoplasmic inclusions (NCI) in the form of Lewy bodies (LB). α-Synuclein is a small pre-synaptic protein which ensures the normal functioning of dopamine transporter and tyrosine hydroxylase (Kovacs et al 2008). It normally exists in a relatively unfolded state and is highly soluble, but in PD undergoes a conformational change to insoluble amyloid fibrils that form a major component of the LB. Hence, DPD is a synucleinopathy, a molecular group of disorders which also includes dementia with Lewy bodies (DLB) and multiple system atrophy (MSA) (Spillantini et al 1998).

Recent studies have questioned the extent to which the density and distribution of LB may account for the clinical symptoms of DPD (Duyckaerts et al 2010) and have demonstrated a significantly more complex synucleinopathy in cortical and limbic regions (Saito et al 2003). In addition to α-synuclein-immunoreactive LB, DPD cases also exhibit Lewy neurites (LN), and Lewy grains (LG), the latter resembling the argyrophilic grains (AG) commonly observed in several conditions including argyrophilic grain disease (AGD) (Braak and Braak 1998, Tolnay et al 1999, Zhukareva et al 2002), Alzheimer's disease (AD) (Sabbagh et al 2009), and elderly cognitively normal brains (Ding et al 2006, Josephs et al 2008).

Occasionally, α-synuclein and tau-immunoreactive grains occur together in the same case (Seno et al 2000). A number of DPD cases have few LB or LN but substantial densities of LG, raising the question as to the relative importance of these pathologies (Oinas et al 2010). Hence, the present study quantified LB, LN, and LG, together with vacuoles, neurons, abnormally enlarged neurons (EN), and glial cell nuclei with the following specific objectives: (1) to determine the relative abundance of LB, LN, and LG in various cortical and limbic regions, (2) the relative importance of EN and vacuoles in the pathology of DPD, (3) to compare densities of the pathology in the upper and lower laminae, (4) to measure the degree of correlation among LB, LN, and LG, and (5) using principal components analysis (PCA) (Armstrong et al 2010), to determine the degree of heterogeneity among cases.

Materials and Methods

Cases

DPD cases (n = 15, mean age 74.13 years, SD = 5.74) (Table 2) were sequentially collected autopsy cases from patients evaluated by movement disorder specialists at the Movement Disorders Center at Washington University School of Medicine in St. Louis (Kotzbauer et al 2012). All patients had a clinical diagnosis of idiopathic PD based on modified United Kingdom Parkinson Disease Society Brain Bank clinical diagnostic criteria and had a clear clinical response to levodopa (Braak et al 2004). Age at PD onset was determined by chart review and defined by onset of motor symptoms. Dementia was determined by clinical assessment and defined as cognitive dysfunction sufficiently severe to impair activities of daily living. In addition, eight control cases (mean age 77.25 years, SD = 7.38) which had no neurological or psychiatric histories were studied.

Neuropathology

These studies were approved by the local Institute Review Board (Human Studies Committee, Washington University School of Medicine) and were carried out according to the 1995 Declaration of Helsinki (as modified Edinburgh, 2000). After death, the next of kin provided written consent for brain removal and retention for research studies. Brains were fixed in 10% neutral buffered formalin for at least two weeks, paraffin-embedded, and sections cut at 6 μm. For this study, blocks were taken from frontal lobes to study the middle frontal gyrus (MFG), anterior cingulate gyrus (CG), and temporal lobes to study the entorhinal cortex (EC), amygdala, and hippocampus. Histologic stains included hematoxylin and eosin and modified Bielschowsky silver impregnation. Immunohistochemistry was performed using the following antibodies: Aβ (10D5, 1:100,000; Elan Pharmaceuticals, San Francisco, CA), phosphorylated tau (PHF-1, 1:500; supplied by Dr. Peter Davies, Albert Einstein Medical School, Bronx, NY), ubiquitin (Dako, Glostrup, Denmark) and phosphorylated α-synuclein (1:10,000; Wako Chemicals USA Inc., Richmond, VA), and phosphorylated TDP-43 (pTDP-43, 1: 40,000; Cosmo Bio Inc., Carlsbad, CA). Lewy body stage was assessed using a PD staging scale (range: 0, 1–6) (Braak et al 2003, 2004) and the McKeith et al. staging scale (McKeith et al 1996, McKeith et al 2005). AD pathological changes were rated using an β-amyloid (Aβ) plaque stage (range: 0, A–C), and NFT tangle (tauopathy) stage (range: 0, I to VI) (Braak and Braak 1991, Braak et al 2006). Diffuse and neuritic plaques were also assessed and cases were classified according to the

neuropathologic criteria of Khachaturian (Khachaturian 1985), the Consortium to Establish a Registry for AD (CERAD) (Mirra et al 1991), and the National Institute on Aging (NIA) and Reagan Institute (Ball et al 1997).

Morphometric methods

In each cortical region, the densities of LB, LN, LG, vacuoles, neurons, EN, and glial cell nuclei were measured along a strip of tissue (3200 to 6400 μm in length) parallel to the pia mater, using 250 × 50 μm sample fields arranged contiguously (Armstrong 2003). The sample fields were located both in the upper (approximating to laminae II/III) and lower (approximating to laminae V/VI) cortex, the short edge of the sample field being orientated parallel with the pia mater and aligned with guidelines marked on the slide. Hence, a standard sample field was used regardless of the degree of brain atrophy and this will inevitably effect which laminae are included in the sample. In the majority of cases, the upper and lower sample fields quantified lesions in laminae II and part of lamina III and in laminae V/VI respectively. In some of the longer duration cases, however, with a greater degree of brain atrophy, the upper sample fields could include a greater proportion of lamina III and part of lamina IV. Similarly in laminae V/VI of longer duration cases, the field would extend into the adjacent white matter and these density counts were corrected for the smaller field size.

It is possible that the pathology of DPD extends across cortical laminae from pia mater to white mater and is not confined to the regions of upper and lower laminae studied. To investigate this possibility, in a small number of gyri with sufficient densities of inclusions, the distribution of the LB, LN, and LG were studied from pia mater to white matter using methods described previously (Armstrong et al 1997, Armstrong 2003). Hence, five traverses from pia mater to the edge of the white matter were located randomly along each gyrus. All histological features were then counted in 50 × 250μm sample fields arranged contiguously, the larger dimension of the field being located parallel with the surface of the pia mater. An eye-piece micrometer comprised the sample field and was moved down each traverse one step at a time from pia mater to the edge of the white matter. Histological features of the section were used to correctly position the field.

In the hippocampus, the histological features were counted in sectors CA1, CA2, CA3, and CA4; 10 contiguous fields being recorded in each sector. The short dimension of the sample field was aligned with the alveus to sample CA1, CA2, and CA3. Measurements were then continued into sector CA4 using a guideline marked on the slide and which ceased approximately 400 μm from the dentate gyrus fascia. In the dentate gyrus, LB, LN, and LG were quantified in the molecular and granule cell layer. No vacuolation or glial cell nuclei were observed in these regions. In the amygdala, the fields were arranged across the maximum diameter of the basolateral nucleus. All distinct rounded inclusions which were α-synuclein-immunoreactive were counted as LB. LN were thread-like structures and often contorted in shape while small circular structures were identified as LG (Fig 1). Neurons were all cells remaining in the section that could be identified as neurons regardless of their degree of pathology, i.e., cells containing at least some stained cytoplasm in combination with larger shape and non-spherical outline (Armstrong 1996). By contrast, small spherical

or asymmetrical nuclei without cytoplasm, but with the presence of a thicker nuclear membrane and more heterogeneous chromatin, were identified as glial cells. EN had irregularly enlarged perikarya, lacked NCI, had a shrunken nucleus displaced to the periphery of the cell, and a maximum cell diameter of at least three times the diameter of the nucleus (Armstrong 1996). The majority of EN showed evidence of chromatolysis when stained with hematoxylin and eosin, the cytoplasm appearing uniformly red. The number of discrete vacuoles present in the neuropil ('spongiosis') greater than 5 μm in diameter was also recorded in each sample field (Armstrong et al 2001, Armstrong et al 2009). It can be difficult to differentiate microvacuolation of the neuropil from vacuolation around neurons and blood vessels attributable to artifacts of processing. Hence, vacuoles clearly associated with such structures were not counted.

Data analysis

The data were analyzed by analysis of variance (ANOVA) (STATISTICA software, Statsoft Inc., Tulsa, OK, USA). First, the densities of each histological feature in the upper cortical laminae only of neocortical regions (MFG, CG, and EC) were compared with those in each CA sector of the hippocampus (CA1 to 4), the amygdala, and dentate gyrus (granule cell layer and molecular layer). For analysis of the LB, LN, and LG there are 10 regions and 15 cases while for neurons, EN, vacuoles, and glial cells, the dentate gyrus data were omitted resulting in 8 regions and 15 cases. Similar analyses were then carried out but substituting densities in the lower cortical laminae only. Subsequent comparisons among brain regions were made using Fisher's 'protected least significant difference' (PLSD) as a *post-hoc* procedure. Second, numerical densities of each histological feature were compared between upper and lower regions of the MFG, CG, and EC using two-factor, split-plot ANOVA (linear model: $x_{ijk} = \mu + M_i + Bj + e_{ij} + T_k + (MT)_{ik} + e_{ijk}$) where μ is the mean, B_j are the cases varying from 1 to 15, M_i represent brain region, T_k upper and lower cortex, $(MT)_{ik}$ the interaction between region and cortical lamina and e_{ij} and e_{ikj} the two error terms, e_{ij} for testing the effect of brain region and e_{ijk} for testing the effect of cortical lamina and its interaction with brain region (Snedecor and Cochran 1980, Armstrong and Hilton 2011). Third, the densities of neurons in cortical gyri, amygdala, and averaged over CA sectors of the hippocampus, were compared in control and DPD cases using two-factor, split-plot ANOVA, a similar model to that above.

Fourth, correlations between the densities of the LB, LN, and LG in each brain region were studied using Pearson's correlation coefficient ('r').

Fifth, to study pathological heterogeneity among cases, the data were analysed using principal components analysis (PCA) (Armstrong et al 2010). The result of a PC A is a scatter plot of the fifteen DPD cases in relation to the extracted PC in which the distance between cases reflects their similarity or dissimilarity based on the defining histological features. Such a plot can reveal whether neuropathological variation is continuously distributed or whether discrete clusters of cases are present. To correlate the location of a case on a PC axis with the numerical density of a specific neuropathological feature, correlations (Pearson's 'r') were calculated between the densities of each histological feature (LB, LN, LG, EN, neurons, vacuoles, glial cell nuclei) of each DPD case and the coordinates

of the case relative to the PC1 and PC2. A significant correlation between the density of a feature and PC1, for example, would identify that feature as important in determining the separation of cases along PC1.

Results

The α-synuclein-immunoreactive pathology of DPD is shown in Fig 1. Small numbers of LB are visible scattered over the section while LN and LG are more widespread and uniformly distributed over the section. A small number of vacuoles are also visible.

The numerical densities of the LB, LN, and LG in each brain region, averaged over the fifteen cases, are shown in Fig 2. The single-factor ANOVA suggest significant differences in density of LB were observed among regions when both the upper ($F = 8.71$, $DF = 9,140$; $P < 0.001$) and lower ($F = 8.49$, $DF = 9,140$; $P < 0.001$) cortex data were included in the analysis. Basolateral amygdala had the greatest densities of NCI compared with upper cortical regions, dentate gyrus, and hippocampus. In addition, the density of LB was significantly greater in sectors CA2, CA3, and CA4 compared with the MFG and the CG. Results were similar when lower cortex data were substituted in the analysis. Significant differences in the density of LN were observed among regions in the upper ($F = 8.44$, $DF = 9,140$; $P < 0.001$) and lower ($F = 9.44$, $DF = 9,140$; $P < 0.001$) cortex, sector CA2 having the greatest densities. Significant densities of LN were also recorded in the EC, amygdala, and sector CA3. The results for the LG were similar to those of the LN. The ratio of LN to LB varied from 1.8 in the dentate gyrus molecular layer to 19.2 in the upper laminae of the CG while the ratio of LG to LN varied from 6.3 in the dentate gyrus granule cell layer to 70.2 in the upper laminae of the CG. Apart from the amygdala ($r = -0.63$, $P < 0.01$), brain weight was not correlated with lesion densities.

The numerical densities of the vacuolation, neurons, EN, and glial cell nuclei in each brain region, omitting the dentate gyrus, are shown in Fig 3. The ANOVA suggest there were no significant differences in the density of vacuoles (upper cortex $F = 0.73$, $DF = 7,112$; $P > 0.05$; lower cortex $F = 0.72$, $DF = 7,112$; $P > 0.05$) or EN (upper cortex $F = 1.81$, $DF = 7,112$; $P > 0.05$; lower cortex $F = 1.06$, $DF = 7,112$; $P > 0.05$) among regions. By contrast, densities of neurons differed significantly among regions (upper cortex $F = 3.74$, $DF = 7,112$; $P < 0.01$; lower cortex $F = 2.16$, $DF = 7,112$; $P < 0.05$) with greater numbers of neurons in the MFG compared with the EC and in sector CA1 compared with sectors CA3, CA4 and the amygdala. Similar results were obtained when lower laminae data were included in the analysis except that there were similar numbers of neurons in the MFG, CG, and EC. There were significant differences in the density of glial cell nuclei among regions in the upper ($F = 8.66$, $DF = 7,112$; $P < 0.001$) and lower ($F = 9.15$, $DF = DF = 7,112$; $P < 0.05$) cortex and greatest glial cell densities were observed in the lower cortex of the EC, basolateral amygdala, and sector CA2.

A comparison of neuronal densities in control and DPD cases in various cortical regions, the hippocampus, and amygdala is shown in Table 3. The two-factor ANOVA suggested no overall difference in density of neurons between control and DPD ($F = 1.32$, $DF = 1,21$; $P > 0.05$) but a significant interaction between patient group and brain region ($F = 3.36$, $DF =$

5,105; P < 0.01) suggesting lower neuronal densities in the CG and EC in DPD especially in the lower cortex whereas numbers of neurons were similar in the amygdala and hippocampus.

A comparison of the densities of each histological feature between upper and lower cortex using two-factor ANOVA is shown in Table 4. The densities of LB (F = 0.31, DF = 1,42; P > 0.05) and vacuoles (F = 0.17, DF = 1,42; P > 0.05) did not differ between upper and lower cortex. However, densities of LN (F = 6.19, DF = 1,42; P < 0.01) and LG (F = 6.91, DF = 1,42; P < 0.05) were significantly greater in the upper compared with the lower laminae, the cortical laminae/region interactions suggesting that this was particularly evident for the LN (F = 3.24, DF = 2,42; P < 0.05) in the EC and LG (F = 6.88, DF = 2,42; P < 0.01) in the EC and CG. Neurons exhibited greater densities in the upper compared with the lower cortex (F = 20.09, DF = 1,42; P < 0.001) in all gyri studied and there were significant differences in glial cell density between regions (F = 6.44, DF = 2,42; P < 0.01) and laminae (F = 66.97, DF = 1,42; P < 0.001), greater densities being observed in the lower cortex, especially in the EC.

Changes in density of LB, LN, and LG across the cortex are shown for a single gyrus (Case A, EC) in Fig 4. Low densities of LB were scattered throughout the cortical profile but the relationship between density of LN and LG with distance from the pia mater appeared to be bimodal, the larger density peak being located in the upper cortical laminae.

Correlations (Pearson's 'r') between the densities of LB, LN, and LG in each region are shown in Table 5. LB were positively correlated with LN in 7/13 regions, LB with LG in 5/13, and LN with LG in all 13 regions studied.

A PCA of the density data resulted in the extraction of two PC's accounting for a total of 72.75% of the total variance (PC1 = 57.67%, PC2 = 15.08%). A plot of the 15 cases in relation to PC1 and PC2 is shown in Fig 5 and the correlations between the locations of the cases on the PC and neuropathological variables in Table 6. The data suggest: (1) PC1 positively correlates with the density of LG in the upper and lower laminae of the MFG and the density of EN in the lower laminae of the MFG, (2) PC1 negatively correlates with the densities of LB in CA1, CA2 and CA3, LN and LG in CA2 and CA4, (3) PC2 positively correlates with the densities of LN and LG in CA2 and LG in CA3, and (4) PC2 negatively correlates with LN and LG in the MFG. In addition, there were no significant correlations between the PC and patient age or with LB, NFT, and Aβ stage.

Discussion

The data suggest that DPD is characterized by the presence of LB, LN, and LG, mean densities of the LN and LG being greater than those of LB respectively in all regions. Apart from the amygdala, there were no significant correlations between densities of LB, LN, or LG and brain weight suggesting brain shrinkage is unlikely to have influenced densities. Among brain regions: (1) LB most significantly affected the basolateral amygdala and sector CA3, (2) LN and LG most significantly affected sectors CA2, CA3, and the EC, and (3) MFG, CA1 and the dentate gyrus were the least affected regions. Small numbers of α-

synuclein-immunoreactive rounded inclusions, resembling small LB, were also observed within the dentate gyrus granule cells, which could be associated with pathological changes in the EC, spreading to the dentate gyrus via the perforant path. In addition, all regions had low densities of EN and vacuoles. Where direct comparisons are possible, the density of LB in DPD was similar to that of DLB, i.e., high densities were present in gyri adjacent to the hippocampus and within the hippocampus, greater densities were present in sectors CA2/CA3 compared with CA1 (Armstrong et al 1998).

The densities of the LB, vacuoles, or EN did not differ between upper and lower cortical laminae in DPD whereas both LN and LG occur with greater densities in the upper cortex, especially in the CG and EC, suggesting a specific degeneration of upper laminae in DPD. These results contrast with those of Braak et al (2003) which suggest that LB have an essentially infragranular distribution in sporadic PD. Hence, it is possible that α-synuclein-immunoreactive pathology has a more extensive distribution in the cortex in some DPD cases compared with sporadic PD. By contrast in DLB, LB density was maximal in the lower laminae in the majority of cortical regions examined (Armstrong et al 1997). Glial cell nuclei, occurred at greater density in the lower cortex in DPD consistent with pathology affecting the lower laminae. Hence, pathological change occurs in both upper and lower laminae in DPD but with the upper laminae of frontal and temporal cortex more significantly affected. It is also possible that some of the results are a consequence of the sampling being confined to two regions of cortex, each 250 μm in depth, located in the upper and lower laminae while it is likely that the pathology is more continuously distributed. Nevertheless, data also suggest that in the gyri examined, LB, LN, and LG were often bimodally distributed with peaks of density within the regions examined. A detailed study of the laminar distribution of the pathology in DPD, especially of the vacuolation, would be useful to describe the pattern of cortical degeneration in more detail.

There were positive correlations among the densities of LB, LN, and LG, most notably between the LN and LG suggesting a close relationship between the three pathologies. LB, LN, and LG could be the result of degeneration of the same neurons, LB aggregating in cell bodies and LN and LG in adjacent neurites and synapses respectively. The close correlation between the densities of LN and LG could be the result of their more widespread distribution, whereas LB often occur in more localized clusters. However, the ratios of LN and LG to LB varied considerably between regions suggesting a more complex relationship between these pathologies/ A proportion of LG may represent sections through LN oriented orthogonal to the section. A correlation between diameters of LG and LN widths was observed in some areas supporting this suggestion. Hence, fine structural studies are required to determine the origin and cellular location of the grains. Spongiosis in PD has been correlated with the presence of LB (Braak et al 2003). However, no correlations were observed between the densities of LB and vacuoles in any of the brain regions studied suggesting that the abundance of vacuoles cannot be explained by the density of LB alone.

The results of the PCA suggest the presence of disease heterogeneity among the fifteen cases. The distribution of the cases along PC1 negatively correlate with densities of LB, LN, and LG in the CA sectors of the hippocampus whereas they are positively correlated with cortical LN and LG. Hence, PC1 separates those cases with high densities of α-synuclein-

immunoreactive pathology in the CA sectors of the hippocampus from those with higher densities of α-synuclein pathology in the MFG and EC. Similarly, PC2 separates those cases with high densities of α-synuclein pathology in the MFG and CG from those with higher densities in the CA sectors of the hippocampus. Recent research suggests that pathogenic proteins such as tau and α-synuclein can be secreted from cells, enter other cells, and seed small intracellular aggregates within these cells (Goedert et al 2010, Steiner et al 2011). It was postulated by Hawkes et al (2007) that pathogenic proteins can spread from cell to cell in PD, and hence, the resulting α-synuclein-immunoreactive pathology may exhibit a spatial distribution in different cases which reflects this spread. This hypothesis is supported by the distribution of LB in DLB which exhibit a spatial pattern in the cortex consistent with spread along cortical pathways (Armstrong and Cairns 2012). Hence, separation of cases along the PC could be explained by variations in the anatomical pathways of spread of α-synuclein-immunoreactive pathology either to the frontal cortex or hippocampus and adjacent gyri.

In conclusion, densities of LN and LG were greater than those of LB respectively in all regions, the ratios of LN and LG to LB varying between regions. Densities of the α-synuclein-immunoreactive pathology were significantly greater in amygdala, EC, and sectors CA2 and CA3 of the hippocampus whereas MFG, sector CA1, and the dentate gyrus were least affected. In regions of the cerebral cortex, the density of LB and vacuoles were similar in upper and lower laminae while the densities of LN and LG were greater in the upper cortex. The densities of LB, LN, and LG were significantly positively correlated with each other, especially the LN and LG. PCA suggested DPD cases were heterogeneous with pathology primarily affecting either hippocampus or cortex and may reflect variation in spread of the pathology to affect primarily cerebral cortex or hippocampus.

Acknowledgments

We thank Deborah Carter, Toral Patel, and Lisa Taylor-Reinwald of the Betty Martz Laboratory for Neurodegenerative Research for expert assistance and we thank the families of patients whose generosity made this research possible. Support for this work was provided by grants from the National Institute on Aging of the National Institutes of Health (P50-AG05681, P01-AG03991), National Institute of Neurologic Diseases and Stroke (NS075321, NS41509, NS058714), NIH (ULITR000488), the Hope Center for Neurological Disorders, the Buchanan Fund, the Charles F. & Joanne Knight Alzheimer's Disease Research Centre, the American Parkinson Disease Association (APDA) Advanced Research Centre for Parkinson Disease at Washington University in St Louis, The Greater St Louis Chapter of the APDA, the McDonnell Center for Molecular and Cellular Neurobiology, and the Barnes-Jewish Foundation (Elliot-Stein Family Fund and Parkinson Disease Research Fund).

References

Antal A, Bandini P, Keri S, Bodis-Wollner I. Visuo-cognitive dysfunctions in Parkinson disease. Clin Neurosci. 1998; 5:147–152. [PubMed: 10785841]

Armstrong RA. Correlations between the morphology of diffuse and primitive β-amyloid (Aβ) deposits and the frequency of associated cells in Down's syndrome. Neuropath Appl Neurobiol. 1996; 22:527–530.

Armstrong RA. Quantifying the pathology of neurodegenerative disorders: quantitative measurements, sampling strategies and data analysis. Histopathol. 2003; 42:521–529.

Armstrong RA. Visual signs and symptoms of Parkinson disease. Clin Exp Optom. 2008; 91:129–138. [PubMed: 18271776]

Armstrong RA, Cairns NJ, Lantos PL. Laminar distribution of cortical Lewy bodies and neurofibrillary tangles in dementia with Lewy bodies. Neurosci Res Communs. 1997; 21:145–152.

Armstrong RA, Cairns NJ, Lantos PL. Lewy body and Alzheimer pathology in temporal lobe in dementia with Lewy bodies. Alz Rep. 1998; 1:159–163.

Armstrong RA, Lantos PL, Cairns NJ. Spatial correlations between the vacuolation, prion protein deposits, and neurons in the cerebral cortex in sporadic Creutzfeldt-Jakob disease. Neuropathology. 2001; 21:266–271. [PubMed: 11837532]

Armstrong RA, Ironside J, Lantos PL, Cairns NJ. A quantitative study of the pathological changes in the cerebellum of 15 cases of variant Creutzfeldt-Jakob disease. Neuropathol Appl Neurobiol. 2009; 35:36–45. [PubMed: 19187059]

Armstrong RA, Ellis W, Hamilton RL, Mackenzie IRA, Hedreen J, Gearing M, Montine T, Vonsattel J-P, Head E, Lieberman AP, Cairns NJ. Neuropathological heterogeneity in frontotemporal lobar degeneration with TDP-43 proteinopathy: a quantitative study of 94 cases using principal components analysis. J Neural Transm. 2010; 117:227–239. [PubMed: 20012109]

Armstrong, RA.; Hilton, AC. Statistical Analysis in Microbiology: Statnotes. New Jersey: Wiley Blackwell, Hoboken; 2011.

Armstrong RA, Cairns NJ. Different molecular pathologies result in similar spatial patterns of cellular inclusions in neurodegenerative disease: a comparative study of eight disorders. J Neural Transm. 2012; 119:1551–1560. [PubMed: 22678700]

Ball M, Braak H, Coleman P, Dickson D, Duyckaerts C, Gambetti P, Hansen L, Hyman B, Jellinger K, Markesbery W, Perl D, Powers J, Price J, Trojanowski JQ, Wisniewski H, Phelps C, Khatchaturian JQ. Consensus recommendations for the postmortem diagnosis of Alzheimer's disease. Neurobiol Aging. 1997; 18:S1–S2. [PubMed: 9330978]

Braak H, Braak E. Neuropathological stageing of Alzheimer-related changes. Acta Neuropathol. 1991; 82:239–259. [PubMed: 1759558]

Braak H, Braak E. Argyrophilic grain disease: Frequency of occurrence in different age categories and neuropathologic diagnostic criteria. J Neural Transm. 1998; 105:801–819. [PubMed: 9869320]

Braak H, del Tredici K, Rub U, de Vos RAI, Steur ENHJ, Braak E. Staging of brain pathology related to sporadic Parkinson's disease. Neurobiol Aging. 2003; 24:197–211. [PubMed: 12498954]

Braak H, Ghebremedhin E, Rub U, Bratzke H, Del Tredici K. Stages in the development of Parkinson disease-related pathology. Cell Tissue Res. 2004; 318:121–134. [PubMed: 15338272]

Braak H, Rub U, Del Tredici K. Cognitive changes in sporadic Parkinson disease- a cliniconeuropathological correlation. Nervenheil. 2005; 24:129–136.

Braak H, Alafuzoff I, Arzberger T, Kretzschmar H, Del Tredici K. Staging of Alzheimer disease-associated neurofibrillary pathology using paraffin sections and immunocytochemistry. Acta Neuropathol. 2006; 112:389–404. [PubMed: 16906426]

Ding ZT, Wang Y, Jiang YP, Hashizume Y, Yoshida M, Mimuro M, Inagaki T, Iwase T. Characteristics of alpha-synucleinopathy in centenarians. Acta Neuropathol. 2006; 111:450–458. [PubMed: 16520971]

Duyckaerts C, Sazdovitch V, Seilhean D. Update on the pathophysiology of Parkinson disease. Bull L'Acad Nat Med. 2010; 194:1287–1303.

Goedert M, Clavaguera F, Tolnay M. The propagation of prion-like protein inclusions in neurodegenerative diseases. Trends in Neurosciences. 2010; 33:317–325. [PubMed: 20493564]

Hawkes CH, Del Tredici K, Braak H. Parkinson disease: a dual hit hypothesis. Neuropathol Appl Neurobiol. 2007; 33:599–614. [PubMed: 17961138]

Hughes AJ, Daniel SE, Kilford L, Lees AJ. Accuracy of clinical diagnosis of idiopathic Parkinson disease: a clinic-pathological study of 100 cases. J Neurol Neurosurg Pyschiatr. 1992; 55:181–184.

Josephs KA, Whitwell JL, Parisi JE, Knopman DS, Boeve BF, Geda YE, Jack CR, Petersen RC, Dickson DW. Argyrophilic grains: a distinct disease or an additive pathology? Neruobiol Aging. 2008; 29:566–573.

Khachaturian ZS. Diagnosis of Alzheimer's disease. Arch Neurol. 1985; 42:1097–1105. [PubMed: 2864910]

Kotzbauer PT, Cairns NJ, Campbell MC, Racette BA, Tabbal SD, Perlmutter JS. Pathological accumulation of α-synuclein and Aβ in Parkinson disease patients with dementia. Arch Neurol. 2012; 23:1–6.

Kovacs GG, Milenkovic IJ, Preusser M, Budka H. Nigral burden of alpha-synuclein correlates with striatal dopamine deficit. Move Disord. 2008; 23:1608–1612.

McKeith IG, Galasko D, Kosaka K, Perry EK, Dickson DW, Hansen LA, Salmon DP, Lowe J, Mirra SS, Byrne EJ, Lennox G, Quinn NP, Edwardson JA, INce PG, Bergeron C, Burns A, Miller BL, Lovestone S, Collerton D, Jansen ENH, Ballard C, de Vos RAI, Wilcock GK, Jellinger KA, Perry RH. Consensus guidelines for the clinical and pathologic diagnosis of dementia with Lewy bodies (DLB): report of the consortium on DLB international workshop. Neurology. 1996; 47:1113–1124. [PubMed: 8909416]

McKeith IG, Dickson DW, Lowe J, Emre M, O'Brien JT, Feldman H, Cummings J, Duda JE, Lippa C, Perry EK, Aarsland D, Arai H, Ballard CG, Boeve B, Burn DJ, Costa D, Del Ser T, Dubois B, Galasko D, Gauthier S, Goetz CG, Gomez-Tortusa E, Holliday G, Hansen LA, hardy J, Iwatsubo T, Kalaria RN, Kaufer D, Kenny RA, Korczun A, Kosaka K, Lee VMY, Lees A, Litvan I, Londos E, Lopez OL, Minoshima S, Mijano Y, Molina JA, Mukaetova-Landinska EB, Pasquier F, Perry RH, Schultz JB, Trojanowski JQ, Yamada M. Diagnosis and management of dementia with Lewy bodies: third report of the DLB Consortium. Neurology. 2005; 65:1863–1872. [PubMed: 16237129]

Melzer TR, Watts R, MacAskill MR, Pitcher TL, Livingston L, Keenan RJ, Dalrymple-Alford JC, Anderson TJ. Grey matter atrophy in cognitively impaired Parkinson's disease. J Neurol Neurosurg Psychiatr. 2012; 83:188–194. [PubMed: 21890574]

Mirra S, Heyman A, McKeel D, Sumi S, Crain B, Brownlee L, Vogel F, Hughes J, van Belle G, Berg L. The consortium to establish a registry for Alzheimer's disease (CERAD). II. Standardisation of the neuropathological assessment of Alzheimer's disease. Neurology. 1991; 41:479–486. [PubMed: 2011243]

Oinas M, Paetau A, Myllykangas L, Notkola IL, Kalimo H, Polvikoski T. Alpha-Synuclein pathology in the spinal cord autonomic nuclei associates with alpha-synuclein pathology in the brain: a population-based Vantaa 85+ study. Acta Neuropathol 2010. 2010; 119:715–722.

Rana AQ, Yousuf MS, Naz S. Qa'aty. Prevalence and relation to dementia to various factors in Parkinson disease. Psych Clin Neuro. 2012; 66:64–68.

Sabbagh MN, Sandhu SS, Farlow MR, Veddeis L, Shell HA, Caviness JN, Connor DJ, Sue L, Adler CH, Beach TG. Correlation of clinical features with argyrophilic grains at autopsy. Alz Dis Assoc Disord. 2009; 23:229–233.

Saito Y, Kawashima A, Ruberu NN, Fujiwara H, Koyama S, Sawaki M, Arai T, Nagura H, Yamanouchi H, Hasegawa M, Iwatsubo T, Murayama S. Accumulation of phosphorylated α-synuclein in aging human brain. J Neuropath Exp Neurol. 2003; 62:644–654. [PubMed: 12834109]

Saper CB, Wainer BH, German DC. Axonal and transneural transport in the transmission of neurological disease: potential role in system degenerations, including Alzheimer's disease. Neuroscience. 1987; 23:389–398. [PubMed: 2449630]

Seno H, Kobayashi S, Inagaki T, Yamamori C, Miyaoka T, Horiguchi J, Wada M, Harada T. Parkinson's disease associated with argyrophilic grains clinically resembling progressive supranuclear palsy: an autopsy case. J Neural Sci. 2000; 178:70–74.

Snedecor, GW.; Cochran, WG. Statistical Methods. Ames, Iowa USA: Iowa State University Press; 1980.

Spillantini MG, Crowther RA, Jakes R, Cairns NJ, Lantos PL, Goedert M. Filamentous alpha-synuclein inclusions link multiple system atrophy with Parkinson disease and dementia with Lewy bodies. Neurosci Lett. 1998; 251:205–208. [PubMed: 9726379]

Steiner JA, Angot E, Brunden P. A deadly spread: cellular mechanisms of α-synuclein transfer. Cell Death and Differ. 2011; 18:1425–1433.

Tolnay M, Monsch AU, Staehelin HB, Probst A. Argyrophilic grain disease: a disorder distinct from Alzheimer's disease. Pathologe. 1999; 20:159–168. [PubMed: 10412175]

Voipicelli-Daley LA, Luk KC, Patel TP, Tanik SA, Eiddle DM, Stieber A, Meaney DF, Trojanowski JQ, Lee VMY. Exogenous alpha-synuclein fibrils induce Lewy body pathology leading to synaptic dysfunction and neuron death. Neuron. 2011; 72:57–71. [PubMed: 21982369]

Willis AW, Shootman M, Kung NH, Evanoff B, Perlmutter JS, Racette B. Predictors of survival in Parkinson disease among United States Medicare beneficiaries. Arch Neurol. 2012; 69:601–607. [PubMed: 22213411]

Zhukareva V, Shah K, Uryu K, Braak H, del Tredici K, Sundarraj S, Clark C, Trojanowski JQ, Lee VMY. Biochemical analysis of tau proteins in argyrophilic grain disease, Alzheimer's disease and Pick's disease: a comparative study. Am J Pathol. 2002; 161:1135–1141. [PubMed: 12368187]

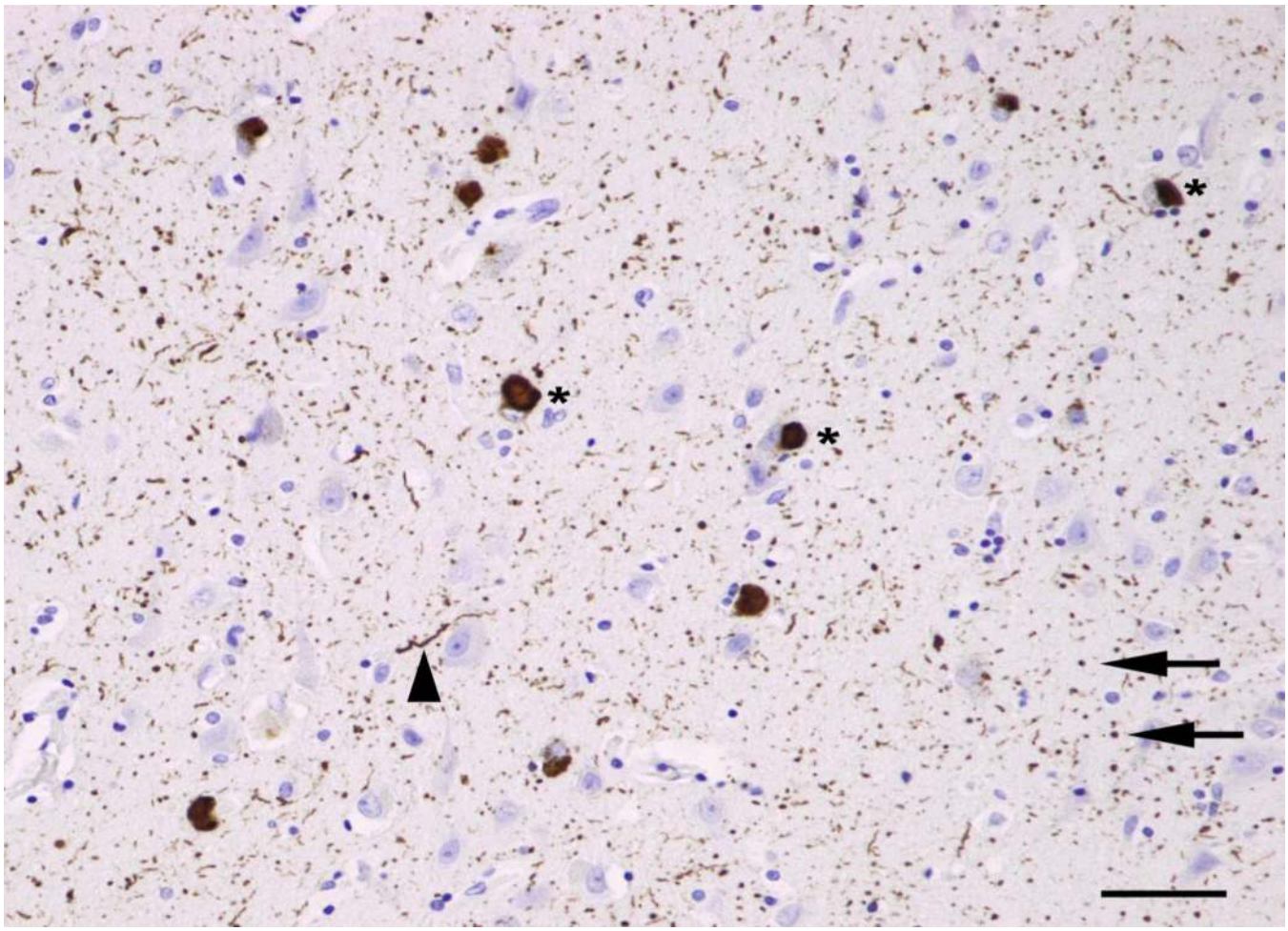

Fig 1.

Typical examples of α-synuclein-immunoreactive pathology in dementia associated with Parkinson's disease (DPD): Lewy bodies (LB*), Lewy neurites (LN, arrow heads), and Lewy grains (LG, arrows) (α-synuclein immunohistochemistry, haematoxylin, bar = 50μm)

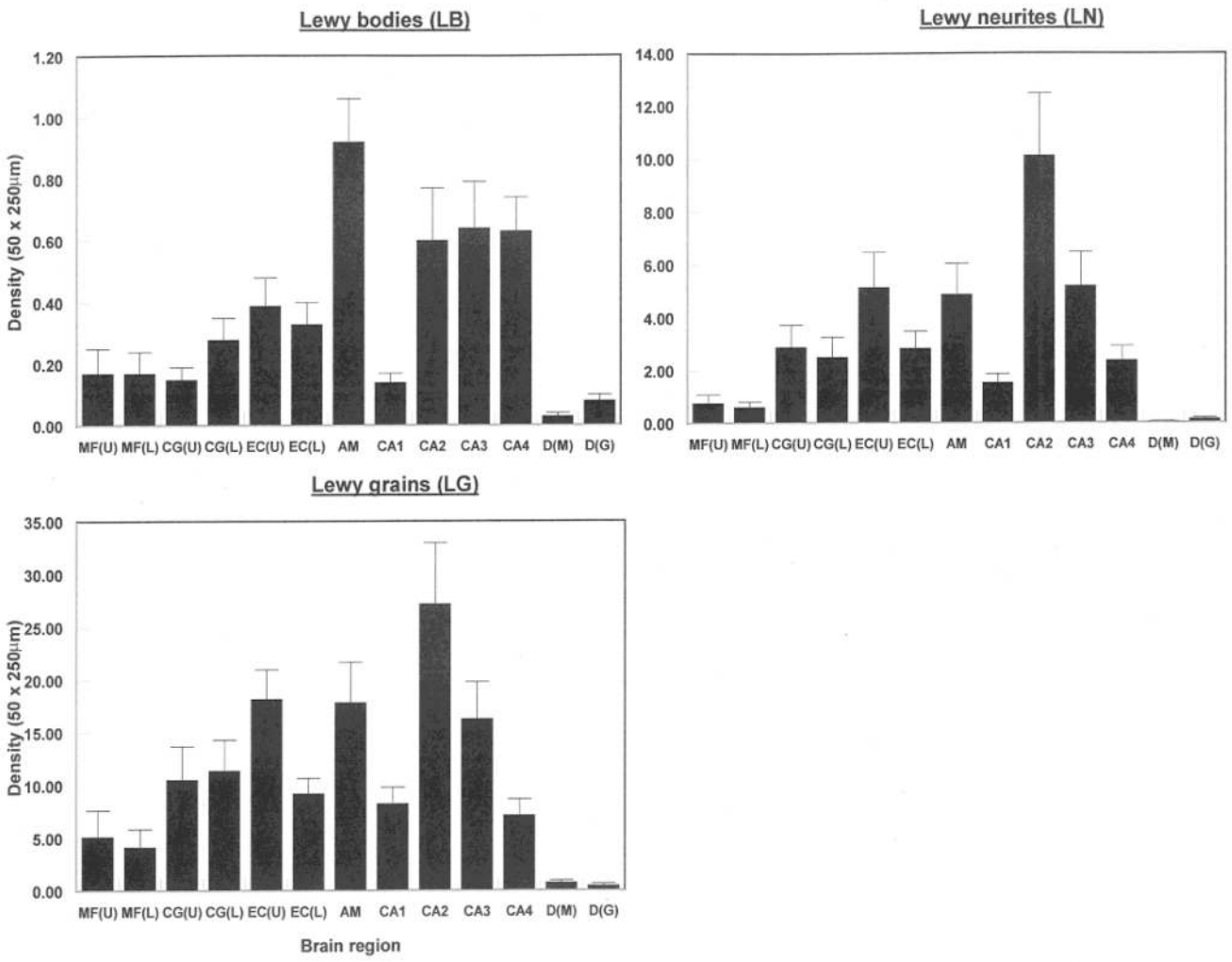

Fig 2.

Densities of α-synuclein-immunoreactive lesions (LB, LN, and LG) in various brain regions (MF = middle frontal cortex, CG = cingulate gyrus, EC = entorhinal cortex, CA1/4 = sectors of the hippocampus, DG = dentate gyrus, ML = molecular layer, GCL = granule cell layer, AM = basolateral amygdala, U = Upper cortex, L = Lower cortex) in fifteen cases of dementia associated with Parkinson's disease (DPD). Analysis of variance (ANOVA): One-way, (Upper cortical laminae, CA1-2, DG, AM): Between brain regions LB $F = 8.71$ ($P < 0.01$); LN $F = 8.44$ ($P < 0.001$), LG $F = 8.31$ ($P < 0.001$); One-way, (Upper cortical laminae, CA1-4, DG, AM): Between brain regions LB $F = 8.49$ ($P < 0.01$); LN $F = 9.44$ ($P < 0.001$), LG $F = 8.82$ ($P < 0.001$)

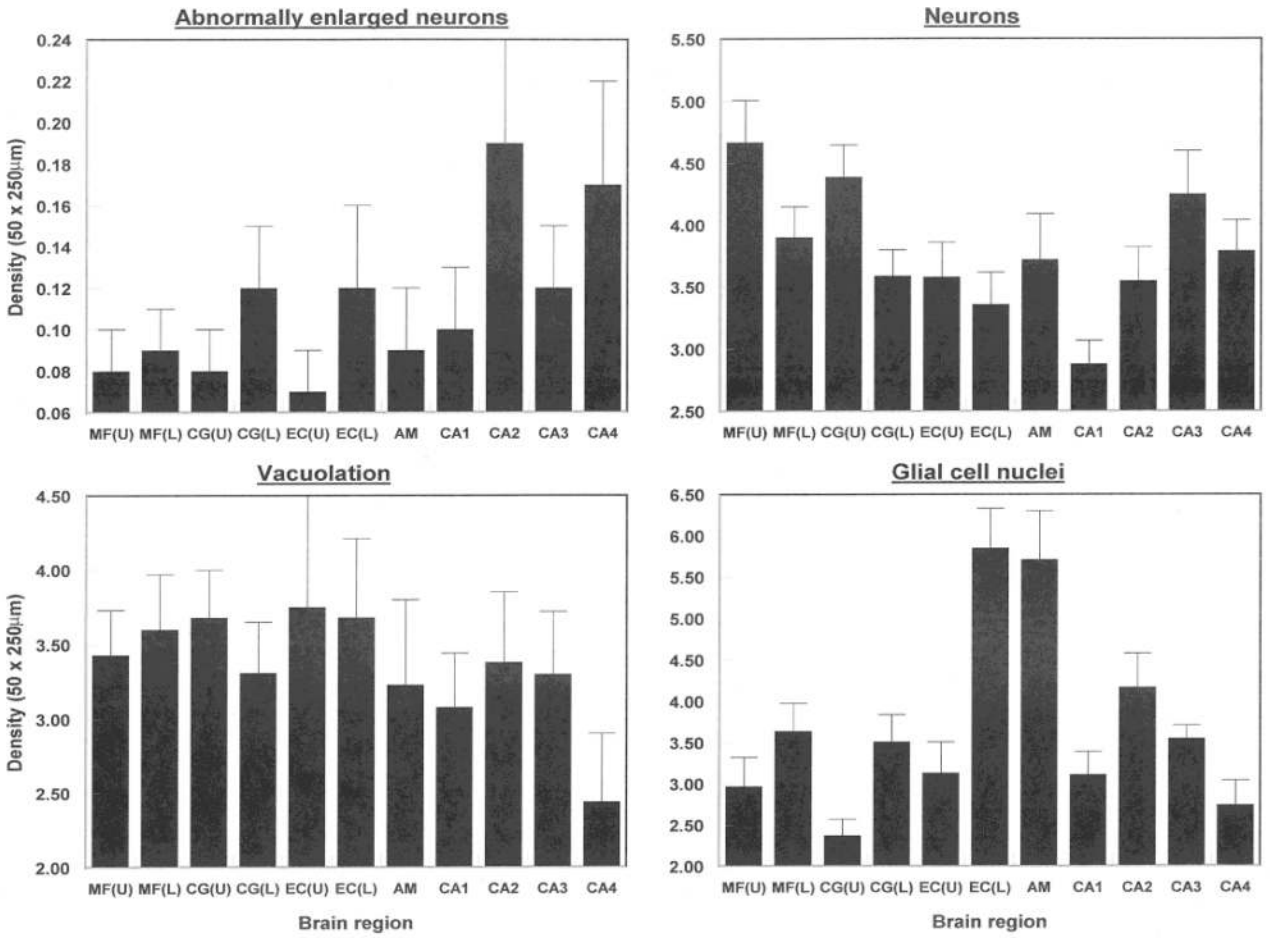

Fig 3.

Densities of vacuoles, abnormally enlarged neurons (EN), neurons, and glial cell nuclei in the upper and lower laminae in in various brain regions (MF = middle frontal cortex, CG = cingulate gyrus, EC = entorhinal cortex, CA1/4 = sectors of the hippocampus, DG = dentate gyrus, ML = molecular layer, GCL = granule cell layer, AM = basolateral amygdala, U = Upper cortex, L = Lower cortex) in fifteen cases of dementia associated with Parkinson's disease (DPD). Analysis of variance (ANOVA): (Upper cortical laminae, CA1-4, AM): Between brain regions EN $F = 1.81$ ($P < 0.05$); neurons $F = 3.74$ ($P < 0.01$), Vacuoles $F = 0.73$ ($P > 0.05$), GL $F = 8.66$ ($P < 0.001$); (Lower cortical laminae, CA1-4, AM): Between brain regions EN $F = 1.06$ ($P < 0.05$); neurons $F = 2.16$ ($P < 0.05$), Vacuoles $F = 0.72$ ($P > 0.05$), GL $F = 9.15$ ($P < 0.001$)

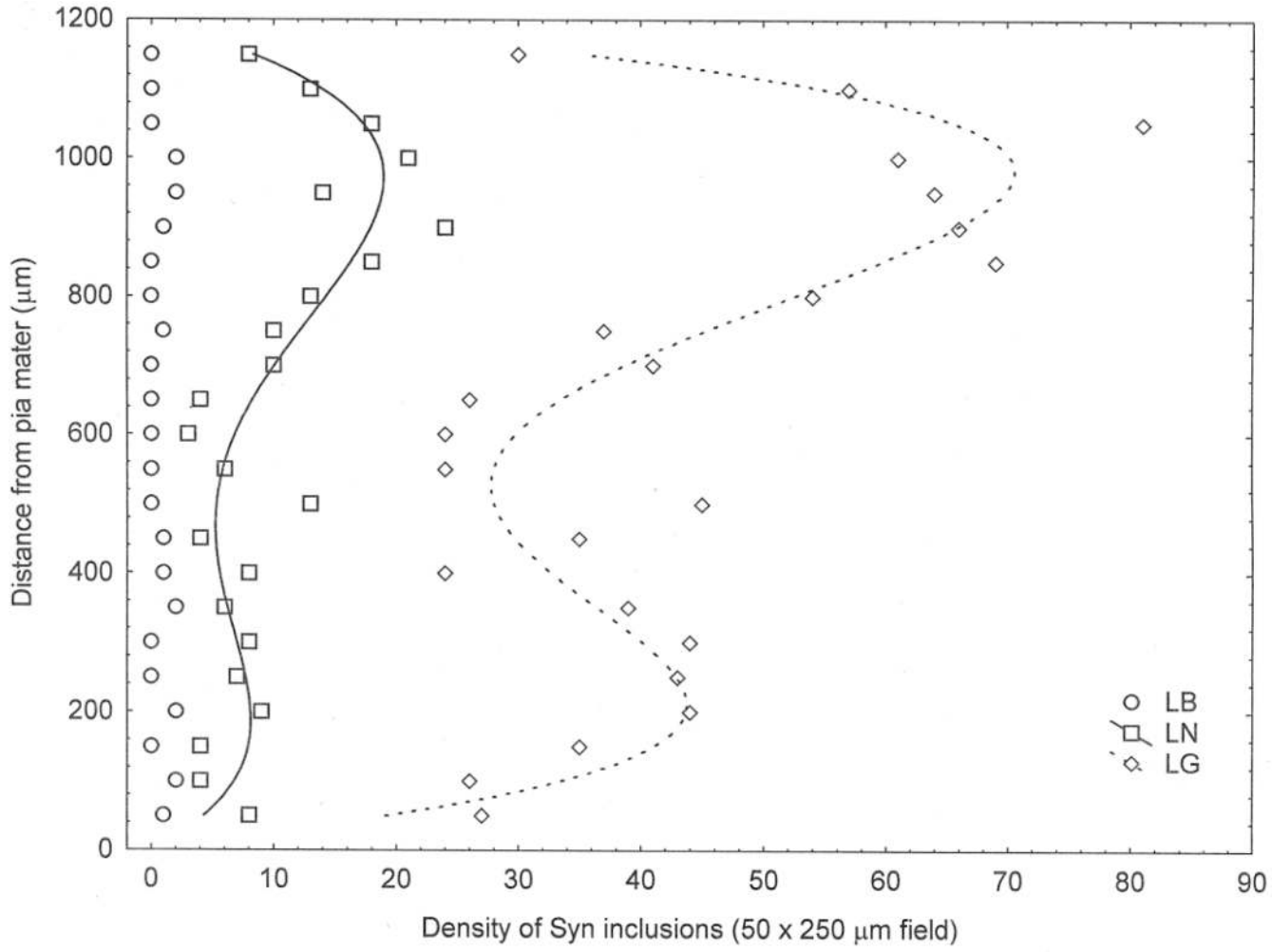

Fig 4.

Examples of the distribution of LC, LN, and LG across the cortex from pia mater to white mater in the entorhinal cortex (EC) of a case of dementia associated with Parkinson's disease (DPD)

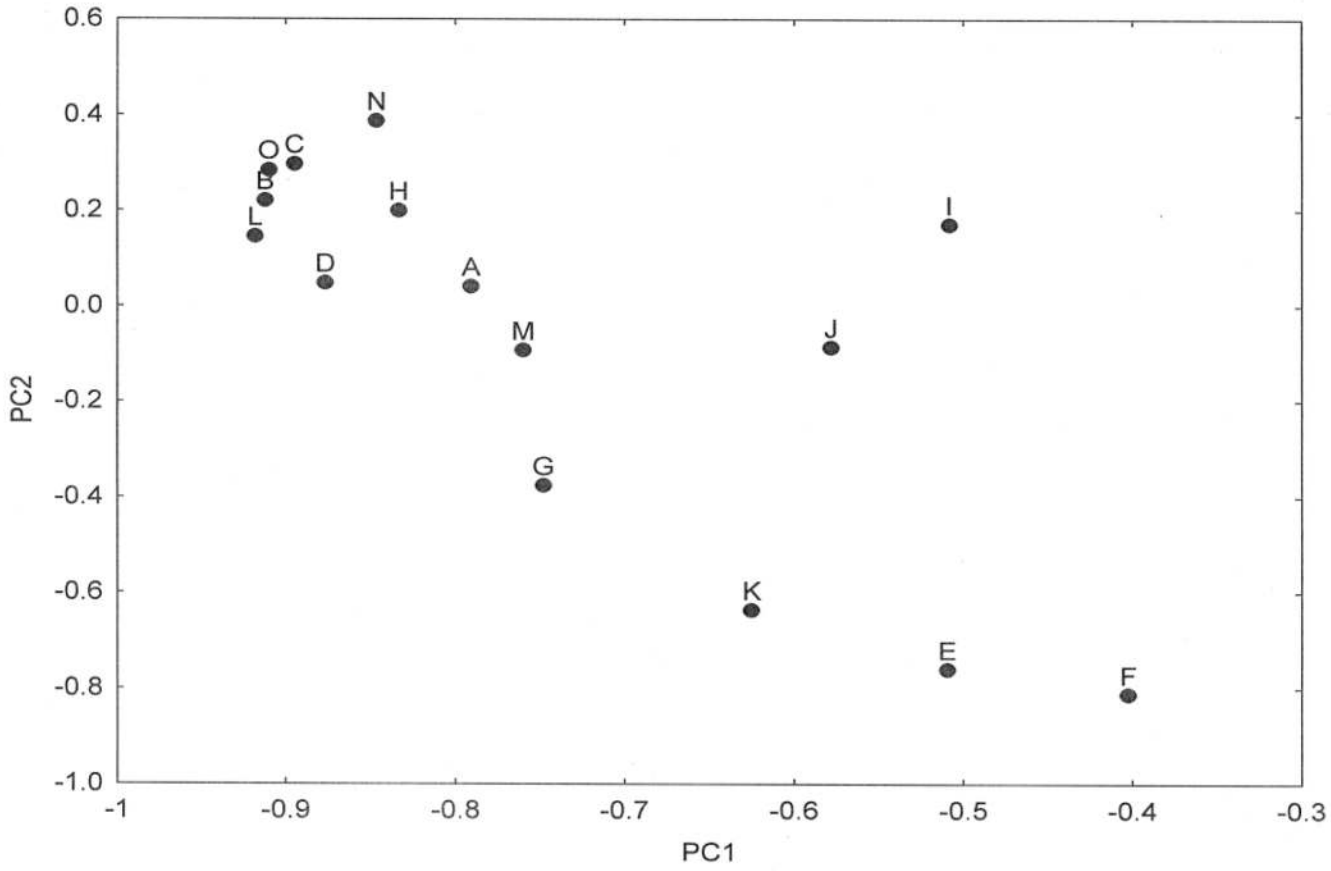

Fig 5.

Principal components analysis (PCA) of fifteen cases of dementia associated with Parkinson's disease (DPD) based on all histological variables. A plot of cases in relation to PC1 and PC2

Table 1

List of abbreviations used in the text

Aβ	β-amyloid
AD	Alzheimer's disease
AG	Argyrophilic grains
AGD	Argyrophilic grain disease
ANOVA	Analysis of variance
CA	Cornu Ammonis
CERAD	Consortium to Establish a Registry of Alzheimer's Disease
CG	Cingulate gyrus
DLB	Dementia with Lewy bodies
DPD	Dementia associated with Parkinson's disease
EC	Entorhinal cortex
EN	Abnormally enlarged neurons
LB	Lewy bodies
LN	Lewy neuritis
LG	Lewy grains
MFG	Middle frontal gyrus
MSA	Multiple system atrophy
NCI	Neuronal cytoplasmic inclusion
NIA	National Institute on Aging
PC	Principal component
PCA	Principal components analysis
PD	Parkinson's disease
pTDP-43	Phosphorylated TDP-43
PHG	Parahippocampal gyrus
SN	Substantia nigra

Table 2

Demographic features, disease stage, and gross brain weight (BW) of the fifteen dementia associated with Parkinson's disease (DPD) cases studied.

Case	Gender	Age	LB	NFT	Aβ	BW(gm)
A	F	82	6	3	0	1210
B	M	80	6	3	C	1360
C	M	78	6	4	A	1330
D	M	79	6	1	A	1260
E	M	71	6	2	C	1540
F	M	78	6	4	C	1320
G	M	76	6	1	A	1370
H	M	67	6	1	C	1550
I	M	67	6	1	C	1470
J	F	73	6	1	0	1600
K	M	76	6	4	B	1130
L	M	77	6	1	B	1450
M	M	64	5	1	C	1290
N	F	66	6	1	A	1120
O	M	78	6	3	B	1230

Abbreviations: M = Male, F = Female, LB = Lewy body stage, NFT = Neurofibrillary tangle stage, Aβ = β-amyloid stage

J Neural Transm. Author manuscript; available in PMC 2015 February 01.

Table 3

A comparison of the densities (50 × 250 μm field, SEM in parentheses) of neurons in various cortical regions (MFG = middle frontal cortex, CG = cingulate gyrus, EC = entorhinal cortex), the hippocampus, and amygdala in control cases and dementia associated with Parkinson's disease (DPD)

Brain region	Laminae	Control	DPD
MFG	Upper	5.32 (0.77)	4.66 (0.34)
MFG	Lower	4.53 (0.94)	3.89 (0.25)
CG	Upper	5.19 (0.99)	4.39 (0.26)
CG	Lower	5.22 (0.83)	3.58 (0.27)
EC	Upper	3.66 (0.41)	3.57 (0.27)
EC	Lower	4.29 (0.40)	3.35 (0.26)
Amygdala	BL	3.81 (0.22)	3.71 (0.37)
Hippocampus	CA1-CA4	3.68 (0.22)	3.62 (0.28)

ANOVA: Between Control/DPD $F = 1.32$ ($P > 0.05$), Between regions $F = 9.07$ ($P < 0.001$), Interaction $F = 3.36$ ($P < 0.01$)

Table 4

Summary of the results of two-factor analyses of variance (ANOVA) of the densities of histological features in the upper and lower cortex in cases of dementia associated with Parkinson's disease (DPD) (Data are 'F' ratios from two factor, split-plot analysis of variance (ANOVA).

	Factorial effect		
Histological feature	**Brain region**	**Upper/Lower cortex**	**Interaction**
Lewy bodies	F = 2.51	F = 0.31	F = 1.39
Lewy neurites	F = 5.69**	F = 6.19*	F = 3.24*
Lewy grains	F = 4.14*	F = 6.91**	F = 6.88**
Enlarged neurons	F = 0.26	F = 3.12	F = 0.49
Neurons	F = 2.89	F = 20.09***	F = 1.97
Vacuoles	F = 0.08	F = 0.17	F = 0.47
Glial cell nuclei	F = 6.44**	F = 66.97***	F = 11.24***

* P < 0.05;

** P < 0.01;

*** P < 0.001.

Table 5

Significant correlations (Pearson's 'r') between the densities of Lewy bodies (LB), Lewy neurites (LN), and Lewy grains (LG), in each brain region (MFG = middle frontal gyrus, CG = cingulate gyrus, EC = entorhinal cortex, CA1/4 = sectors of the hippocampus (HC), DG = dentate gyrus, ML = molecular layer, GCL = granule cell layer, AM = amygdala, BL = basolateral nucleus) in dementia associated with Parkinson's disease (DPD).

Region	Laminae/ Region	LB/LN	LB/LG	LN/LG
MFG	Upper	-	-	0.64**
	Lower	-	-	0.92***
CG	Upper	0.70**	0.89***	0.89***
	Lower	-	-	0.79***
EC	Upper	-	-	0.81***
	Lower	0.79***	0.70**	0.85***
HC	CA1	0.61*	-	0.77***
	CA2	0.54*	-	0.94***
	CA3	0.66**	0.62*	0.94***
	CA4	0.54*	0.55*	0.96***
DG	ML	-	-	0.62**
DG	GCL	-	-	0.56*
AM	BL	0.92***	0.73**	0.76**

* $P < 0.05$;

** $P < 0.01$;

*** $P < 0.001$; (-) indicates regions with non-significant correlations.

Table 6

Correlations (Pearson's 'r') between the Syn-immunoreactive pathological features (LB = Lewy bodies, LN = Lewy neurites, LG = Lewy grains), EN = abnormally enlarged neurons, N = neurons, V = vacuolation, GL = Glial cell nuclei) and the first two principal components (PC) in various brain regions (MFG = middle frontal gyrus, CG = cingulate gyrus, EC = entorhinal cortex, CA1/4 = sectors of the hippocampus, DG = dentate gyrus, ML = molecular layer, GCL = granule cell layer, AM = basolateral amygdala in dementia associated with Parkinson's disease (DPD).

Region	PC	LB	LN	LG	EN	N	V	GL
MFG-U	1	–0.11	0.40	0.65**	0.20	–0.20	0.47	–0.05
	2	0.09	–0.65**	–0.73**	–0.09	0.21	–0.15	0.09
MFG-L	1	0.02	0.57*	0.68**	0.59**	–0.13	0.33	0
	2	–0.05	–0.71**	–0.80***	–0.51*	0.10	–0.15	–0.07
CG-U	1	0.32	0.12	0.38	0.36	–0.34	0.49	0.27
	2	–0.59**	–0.40	–0.67*	–0.61**	0.35	–0.01	0.07
CG-L	1	0.04	0.12	0.49	0.40	–0.05	0.11	0.23
	2	–0.05	–0.31	–0.71*	–0.28	0.12	0.30	–0.10
EC-U	1	–0.10	–0.32	–0.16	0.52*	–0.27	–0.01	0.25
	2	–0.20	0.01	–0.29	–0.65**	0.41	–0.11	–0.37
EC-L	1	–0.17	–0.33	–0.38	0	–0.14	0.05	0.03
	2	–0.12	0.03	0.13	–0.08	0.38	–0.07	–0.22
CA1	1	–0.70**	–0.51	–0.56*	–0.03	–0.36	0.29	–0.25
	2	0.50	0.26	0.42	0.36	0.58*	–0.19	0.21
CA2	1	–0.61**	–0.75**	–0.79***	–0.43	0.50	0.48	–0.45
	2	0.46	0.68**	0.72**	0.45	–0.26	–0.54*	0.34
CA3	1	–0.60	–0.49	–0.54	0.42	–0.08	0.17	–0.32
	2	0.45	0.48	0.61*	–0.07	0.30	–0.25	0.35
CA4	1	–0.39	–0.61**	–0.67**	–0.32	–0.04	0.09	–0.05
	2	0.32	0.47	0.55*	0.29	0.09	–0.32	0.01
DG-ML	1	–0.04	–0.20	–0.26	-	-	-	-
	2	0.52**	–0.07	0.06	-	-	-	-
DG-GCL	1	–0.35	–0.57**	–0.35	-	-	-	-

Region	PC	LB	LN	LG	EN	N	V	GL
	2	0.27	0.40	0.36	-	-	-	-
AM	1	–0.02	–0.13	0.02	–0.19	–0.03	0.24	–0.24
	2	–0.25	–0.20	–0.41	0.10	0.25	–0.26	0.15

* P < 0.05;

** P < 0.01;

*** P < 0.001; (-) represents pathology not measured